NCTSPM

NATIONAL CENTER FOR TRANSPORTATION SYSTEMS PRODUCTIVITY AND MANAGEMENT
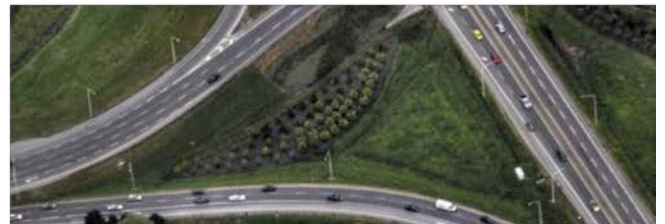
Evaluation of Design Loads for Concrete Bridge Rails

Contract # DTRT12GUTC12 with USDOT Office of the Assistant Secretary for Research and Technology (OST-R)

Final Report

March 2016

Principal Investigator: Dr. Dean Sicking, University of Alabama at Birmingham

**National Center for Transportation Systems
Productivity and Management**
O. Lamar Allen Sustainable Education Building
788 Atlantic Drive, Atlanta, GA 30332-0355
P: 404-894-2236   F: 404-894-2278
nctspm@ce.gatech.edu   nctspm.gatech.edu

Evaluation of Design Loads for Concrete Bridge Rails

By

Kevin Schrum, Ph.D.
Instructor, Research Engineer
University of Alabama at Birmingham
School of Engineering
371A Hoehn Engineering Building
1075 13th Street South
(205) 934-8470
kschrum@uab.edu

Dean Sicking, Ph.D., P.E.
Professor, Associate VP for Product Development
University of Alabama at Birmingham
School of Engineering
371B Hoehn Engineering Building
1075 13th Street South
(205) 934-8492
dsicking@uab.edu

Nasim Uddin, PhD, P.E., F.ASCE
Professor
University of Alabama at Birmingham
School of Engineering
321 Hoehn Engineering Building
1075 13th Street South
(205) 934-8432
nuddin@uab.edu

3/1/2016

DISCLAIMER

This report was completed with funding from the Alabama Department of Transportation (DOT). The contents of this report reflect the view and opinions of the authors who are responsible for the facts and the accuracy of the data presented herein. The contents do not necessarily reflect the official views or policies of the Alabama DOT or any other governing body. This report does not constitute a standard, specification, or regulation.

ABSTRACT

Crash test standards for bridge rails now adhere to the Manual for Assessing Safety Hardware (MASH), which describes the required vehicles for Test Level 4 (TL-4) and Test Level 5 (TL-5). TL-5 conditions have not been changed relative to the predecessor standard, but the TL-4 vehicle has increased in mass, prompting some to consider whether or not the AASHTO transverse design loads on bridge rails should also increase. Increased transverse loads would lead to heavier bridge rails and stronger deck overhangs, which will increase the costs for bridge construction. This report presents a modified approach to the yield line method that accounts for momentum transfer and concrete rail deformation to determine barrier capacities. Also, the modified approach was used to examine bridge rails that have already been approved by the Federal Highway Administration or that have been crash tested in a controlled laboratory setting. Preliminary computer simulations were also carried out to corroborate the calculations of the modified yield line method by comparing the estimated internal energy of the deformed vehicle. The simulations demonstrated that the modified yield line method was accurate. In addition, applying the analysis to one bridge rail that was structurally inadequate in a crash test, it was shown that the current AASHTO design loads are appropriate, even for MASH impact conditions.

Table of Contents

Table of Figures

Table of Tables

1. INTRODUCTION

1.1. *Background*

In the mid to late 1970s, T.J. Hirsch developed what is now called the Yield Line Method (YLM) to analyze the crash test results of some Texas bridge rails that were impacted with buses and trucks [1]. The bridge deck was not included in the analysis. The bridge rail itself was treated as a rigid object that was defined by sections that were separated by yield lines. Often, a vertical crack formed at the point of contact, and two angled cracks extended from the bottom of the vertical crack in the upstream and downstream directions. The YLM attempts to estimate the bridge rails capacity assuming that these yield lines represent a state of failure. To do so, three moment capacities must be defined: (1) beam; (2) wall; and (3) cantilever. For bridge rails with a discernible beam at the top, this first moment capacity would be non-zero, but for a majority of safety shapes, this beam moment capacity is assumed to be zero. The wall moment capacity is defined by both the Whitney stress block of the concrete and the reinforcement design through the cross-section of the bridge rail. The cantilever moment capacity is determined from the stirrup/overhang interface reinforcement, including the spacing the rebar longitudinally as well as the concrete strength and width at the interface between the rail and the deck.

Hirsch analyzed crash test data to determine forces acting on the wall from the vehicle. He then compared his analytic prediction with the data, and when the YLM overpredicted the barrier capacity, Hirsch used engineering judgment to reduce the predicted force from the YLM. With these adjusted results, he recommended the design loads that the American Association of State Highway Transportation Officials (AASHTO) requires in their bridge design specification [37]. The most recent publication recommends transverse design loads of 54 kips and 124 kips for Test Level (TL) 4 and TL-5, respectively. These specifications were believed to apply adequately to the National Cooperative Highway Research Program (NCHRP) Report No. 350 (NCHRP 350) test conditions, which were set forth in 1993 [37]. TL-4 was defined by an impact with an 18,000-lb single-unit truck, whereas TL-5 was defined by an impact with an 80,000-lb semi-tractor trailer.

Hirsch reviewed the equations presented in NCHRP Report 86 [6], as described in Equations 1 through 4. The parameters for these equations can be found in Hirsch's report, and are repeated in Figure 1 and Figure 2. These equations were used to analyze crash test data.

$$avg\ G_{lat} = \frac{V_I^2 \sin^2 \theta}{2g\{AL \sin \theta - B[1 - \cos \theta] + D\}} \tag{1}$$

$$max\ G_{lat} = \frac{\pi}{2}(avg\ G_{lat}) \tag{2}$$

$$avg\ F_{lat} = (avg\ G_{lat})w \tag{3}$$

$$max\ F_{lat} = \frac{\pi}{2}(avg\ F_{lat}) \tag{4}$$
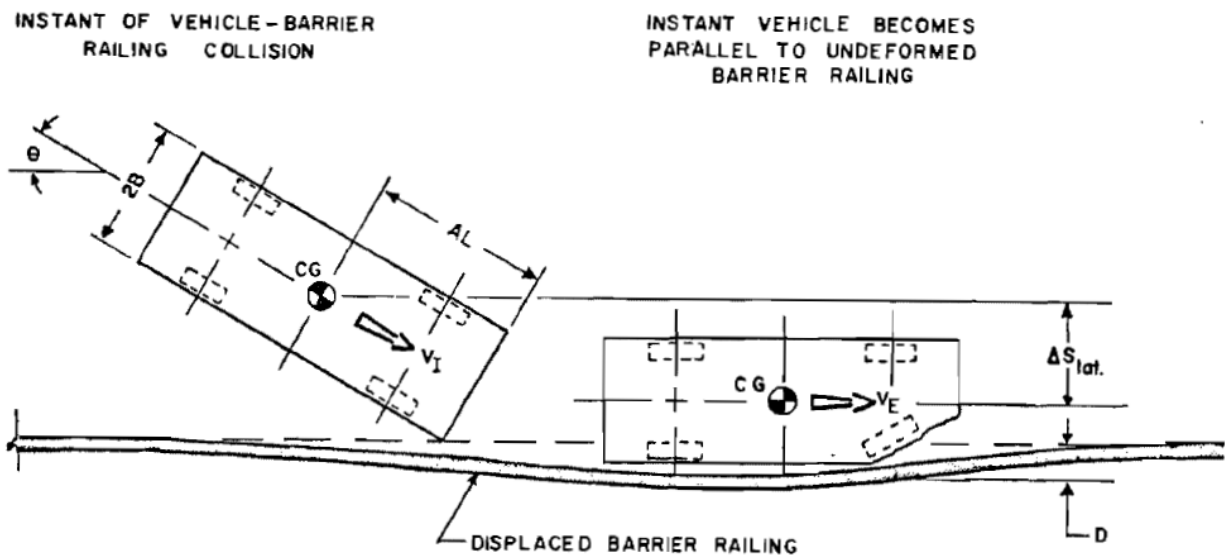
Figure 1. Mathematical Model of Vehicle - Barrier Railing Collision [6]

```
 L = vehicle length (ft);

2B = vehicle width (ft);

 D = lateral displacement of barrier railing (ft)

     assumed as zero for rigid rail;

AL = distance from vehicle's front end to center of mass (ft);
```

V_I = vehicle impact velocity (fps);

V_E = vehicle exit velocity (fps);

θ = vehicle impact angle (deg);

μ = coefficient of friction between vehicle body and barrier railing;

a = vehicle deceleration (ft/sec^2);

g = acceleration due to gravity (ft/sec^2);

m = vehicle mass (lb-sec^2/ft); and

W = vehicle weight (lb).

Figure 2. List of Variable Definitions Used by Hirsch [1]

Then, Hirsch developed the yield line method to predict the strength of a bridge rail based solely on the design of the barrier. Regardless of the barrier type, the impact conditions were illustrated in a similar manner, as seen in Figure 3. For concrete bridge rails, the key components of the analysis were labeled as shown in Figure 4.

w = distributed load, lb/ft or N/m

ℓ = length of distributed load, ft or m

$w\ell$ = total impact load, lb or N
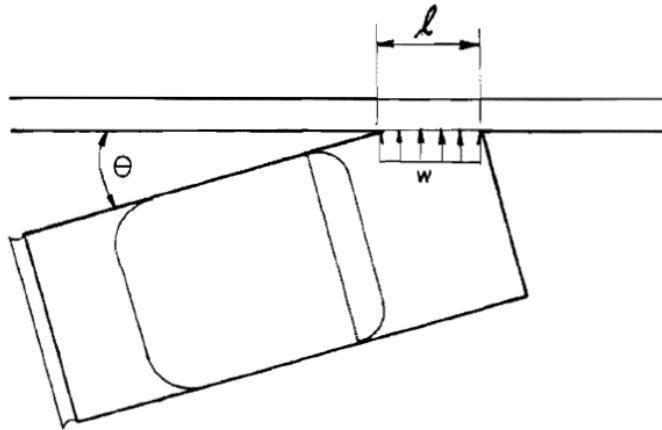
Figure 3. Distribution of Impact Load in Collision with Longitudinal Traffic Rail [1].
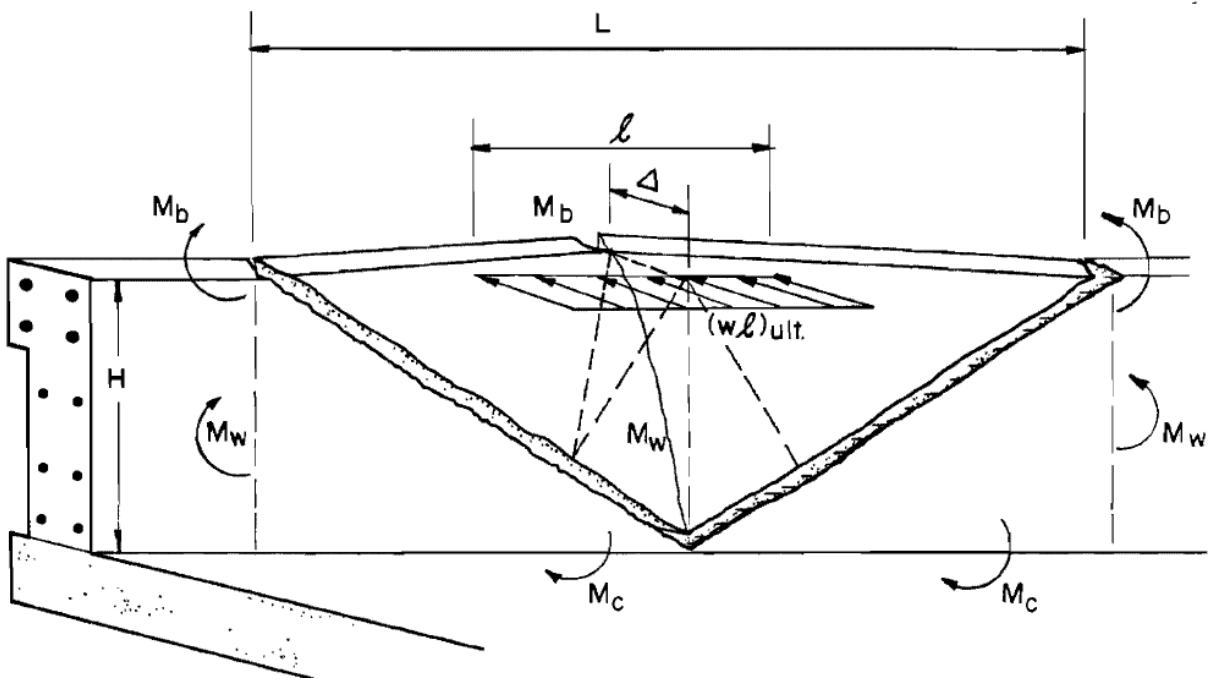
Figure 4. Yield Line Analysis of Concrete Parapet Wall [1].

With these definitions, Hirsch developed his yield line equations to determine the load on the barrier that induced yielding (*wl*) and the length of the yielded portion (*L*), according to Equations 5 and 6, respectively.

$$wl = \frac{8M_b}{L \cdot l/2} + \frac{8M_w H}{L - l/2} + \frac{M_c L^2}{H(L - l/2)} \tag{5}$$

$$L = \frac{l}{2} + \sqrt{\left(\frac{l}{2}\right)^2 + \frac{8H(M_b + M_w H)}{M_c}} \tag{6}$$

Where:

wl = total ultimate load capacity of the wall, kips

l = length of distributed impact load, ft

M_b = ultimate moment capacity of a beam at the top of the wall, kip-ft

M_w = ultimate moment capacity of the wall per foot of wall height, kip-ft/ft

M_c = ultimate moment capacity of the wall cantilever up from the bridge deck per foot of length of wall, kip-ft/ft

H = height of wall, ft

L = critical length of wall failure, ft

Hirsch's work focused on buses and heavy vehicles. Buses fall between test levels of the previous and current crash test standard, in terms of impact severity. The design loads recommended by Hirsch were adopted even after NCHRP 350 test conditions were established in 1993 and remained in effect until 2009.

Since 2009, the *Manual for Assessing Safety Hardware* (MASH) [37] has replaced NCHRP 350, an in many cases, the impact energy was increased to match the modern vehicle fleet. The TL-4 vehicle increased to approximately 22,000 lbs, but the TL-5 vehicle was unchanged. Intuitively, with a larger vehicle, it may be expected that the design load would increase from the NCHRP 350 levels. However, the designs generated from the previous test standard impact conditions have not led to a nationwide pandemic of failing bridge rails. Vehicles have gotten larger, but the bridge rail designs have essentially remained unchanged, with the exception of barrier height. This increase in height was intended to address rollover in taller vehicles, not an increase in transverse load. Despite this observation, some researchers have conducted analyses via the finite element method (computer simulation) to determine what loads are being imparted on bridge rails. Their recommendations were to increase the TL-4

design load to 80 kips and the TL-5 load to at least 160 kips (for barriers shorter than 42 inches) and up to 260 kips (for barriers taller than 42 inches) [37].

1.2. *Problem Statement*

By increasing required design loads, new bridge rails will be wider and carry more steel, making them heavier and more costly. The cost considerations are further compounded when the additional dead load is considered in the design of the overhang deck. Before such magnanimous policy changes are instituted, which could substantially hamper any State highway budget, these design loads need to be examined further.

Particularly, there does not seem to be a large contingency of cases where the bridge rail was insufficient capacity when struck by a large vehicle. That hypothetical bridge rail was most likely designed according to the specifications currently in AASHTO. It is worth noting that the AASHTO design loads were based on some engineering judgment and for vehicle classes that do not directly correspond with NCHRP 350 or MASH test vehicles. As such, it may be possible that the current design loads were already conservative. There hasn't been an illustrated need to increase these design loads yet. However, MASH has only been in place since 2009. Therefore, the possibility exists that the new expected loads, from the larger vehicles, may necessitate an increase in design loads.

In addition to engineering judgment, Hirsch, and almost everyone that has followed after him, made assumptions of rigidity in the barrier and deck. The barrier may be loaded through a large deformed area, especially for the longer semi-tractor trailer vehicles. With the wide variety of barrier shapes and heights, the energy absorption inherent in the bending and rotating of the barrier need to be considered. Also, the current YLM ignores the crush of the vehicle as a source of energy dissipation. Before extremely expensive design policies are implement, each of these components must be analyzed.

1.3. *Objectives*

This research project was intended to determine appropriate concrete bridge rail design loads such that MASH-style vehicles could not cause any structural damage to the rail. To do so, the YLM method was modified to account for momentum transfer between the vehicle and the barrier as well as internal energy due to crush of the vehicle. Finally, with the analysis complete,

this research effort will identify a minimum safety performance for which a crash test occurred and no structural damage was taken by the barrier. Finally, this minimum will be compared to existing capacity requirements and TTIs recommended specifications and will recommend the appropriate design loads that should be adopted as minimum transverse design loads for TL-4 and TL-5 only.

1.4. *Scope*

The proposed recommendations for design loads applies to concrete bridge rails only. It is intended to evaluate the design specifications only, but the methodology may be adapted for new designs, so long as any new bridge rail is thoroughly evaluated and crash tested according to the most recent crash test standard. This research does not apply to post-and-beam style bridge rails because it requires a relatively constant cross-sectional area for mass calculations.

2. RESEARCH APPROACH

2.1. *Develop a Modified YLM*

Hirsch's original formulation of the YLM to evaluate the capacity of bridge rails assumed rigidity in the bridge rail. It also did not account for the crush of the vehicle as a substantial source of energy dissipation. Therefore, the first step in this project was to develop a modified YLM that incorporated barrier deformation and vehicle crush in the analysis.

In the traditional YLM, a critical length of barrier must be determined. Originally, this length was a function of the three moment capacities and the height of the barrier, in addition to the width of the distributed load. Fundamentally, the modified YLM proposed herein relies on many of the same calculations as the traditional YLM, but the primary difference is the way in which the critical length is calculated. This new approach will use linear momentum and internal energy to establish the critical length.

The law of conservation of linear momentum for a perfectly plastic impact between two objects states that the velocity of the two-object system will be equal to the sum of the momentums of the two objects prior to impact divided by the combined mass of the two objects. In this case, the bridge is stationary (initial velocity and momentum are zero), and the new velocity becomes the initial velocity of the truck times the ratio of the truck's mass to the combined mass. The critical length determines the mass of the barrier, since mobilizing the entire bridge rail is generally not possible. In other words, only a portion of the bridge rail moves upon impact with the vehicle. The critical length defines this portion.

Strain energy in the barrier and internal energy in the vehicle are both derived from the law of conservation of linear momentum. The barrier is accelerated, and therefore deformed, thus absorbing energy. The amount of this deformation is dependent on the load, but boundary conditions can be applied to ascertain a specific performance. In this case, the maximum strain in the rebar was not to exceed 6%. Using a simplified deformation shape of the barrier, this strain limit was used to calculate the deformed area of the concrete, which was then used to calculate the strain energy in the barrier.

Next, the reduced velocity of the truck following the inertial momentum transfer was used to calculate a new kinetic energy using the velocity component that was perpendicular to

the barrier. The difference in this new energy and the original impact energy constitutes the change in internal energy of the truck due to crush.

Finally, the Impact Severity (IS) of the truck prior to impact was set equal to the sum of the barrier's strain energy and the vehicles change in internal energy. This equation yields one unknown parameter, the critical length. However, it is a non-linear equation and required iterative numerical methods to calculate the critical length. The resistive capacity of the barrier was then determined as a function of this critical length and other parameters in a simple, linear equation.

2.2. *Analyze Existing Concrete Bridge Rails*

After the modified YLM was mathematically derived, it was applied to numerous existing concrete bridge rails. The concept was that if the barrier had been crash tested, then the test agency would have noted any structural damage to the barrier as a result of the loads imparted from the vehicle to the bridge rail. After determining the barrier's capacity from the modified YLM, the crash test reports for the weakest barriers were reviewed to determine their structural performance in the crash test.

First, all bridge rails considered crashworthy by the Federal Highway Administration (FHWA) were identified, and any associated cross-sectional drawings provided either by the FHWA or by another entity (such as TTI or the New Jersey Turnpike Authority) were gathered. From these drawings, the cross-sectional area was calculated, which is a crucial component in the modified YLM.

The drawings also contained the reinforcement design and details on the compressive strength of the concrete. From these parameters, the moment capacities for each bridge rail were calculated. Generally, the beam moment capacity was zero, so long as no additional beam elements were included at the top of the rail. The wall and cantilever capacities were functions of the longitudinal and shear reinforcement, respectively.

Next, the moment capacities and barrier height were plugged into the modified YLM governing equation, and by the process of iteration, the critical length was calculated. Once this

length was determined, a simple equation was used to determine the resistive capacity of the barrier. These two calculations were dependent on the loading conditions (i.e., TL-4 or TL-5).

2.3. *Energy Verification with LS-DYNA*

The governing equation of the modified YLM contained three components: (1) impact severity; (2) strain energy of the barrier; and (3) the change in internal energy of the truck. All three of these components are linked to one another. The IS is a constant and must be absorbed by the other two components. Hypothetically, if the strain energy of the barrier decreases, then the vehicle's change in internal energy would have to increase.

The balance of this governing equation was investigated by examining the total change in internal energy of truck using LS-DYNA, a non-linear explicit finite element analysis code developed by Livermore Software Technology Cooperation (LSTC). A single unit truck model was publicly available through the archive of the National Crash Analysis Center (NCAC). The bridge rail geometry matched a standard 32-inch New Jersey safety shape bridge rail, which was simulated with a built-in concrete model, *MAT_159. This material model provides the freedom to adjust the compressive strength, average aggregate size, and damage coefficient. This final term was calibrated by comparing a model to physical testing of reinforced concrete beams. These beams were impacted by a bogey vehicle at the Barber Laboratory for Advanced Safety Education and Research (BLASER) in Leeds, AL. With a calibrated concrete material model, the research team could confidently assume that the strain energy in the barrier was accurate. LS-DYNA does not currently provide post-processing for strain energy. Therefore, the internal energy of the vehicle was studied to corroborate the governing equation of the modified YLM.

3. MODIFIED YIELD LINE METHOD

The YLM was modified to determine the critical length of the barrier in a more inclusive way. In particular, the strain energy developed due to the barrier's deflection and the change in internal energy of the vehicle due to its crush were incorporated. The governing principle of the modified yield line method is displayed as Equation 7:

$$(IS) = (SE \ in \ Barrier) + (\Delta IE \ of \ the \ Vehicle) \tag{7}$$

Where:

IS = Impact Severity, kip-ft

SE = Strain Energy, kip-ft

ΔIE = Change in Internal Energy, kip-ft

To understand and assemble the components of Equation 7, a cursory discussion on impact severity, strain energy, momentum, and energy were presented in the sections that follow. Following the description of these elements, Equation 7 will be fully assembled, and the procedure for calculating the new critical length will be provided.

3.1. *Mechanics*

3.1.1. *Impact Severity*

The impact condition shown in Figure 1 includes a mass, velocity, and impact angle for the vehicle. By definition, velocity is a vector, which means it is a speed with a direction. That speed, combined with the vehicle's mass, can be used to calculate the kinetic energy of the vehicle. However, the barrier only resists the perpendicular component of that velocity. Therefore, the energy dissipation required to arrest the vehicle's perpendicular velocity, or become parallel with the barrier, is given by the Impact Severity (IS). Note the constant (1/1000) converts the IS from lb-ft to kip-ft.

$$IS = \frac{1}{2}m(v \sin \theta)^2 \cdot \frac{1}{1000} \tag{8}$$

Where:

m = Mass of the vehicle, lb-ft/s^2 (slugs) = W_T/g

W_T = Weight of the vehicle, lbs

g = Acceleration due to gravity, 32.174 ft/s^2

v = Velocity of the vehicle, ft/s

θ = Impact angle, degrees

3.1.2. Strain Energy

In its most basic form, strain energy is the energy stored by a deformed object. For this project, the strain energy was defined as the external force times the displaced distance of the barrier. This external force was the maximum force the barrier could withstand based on its three moment capacities and its height. The displacement was determined from the maximum strain in the rebar, assuming a maximum of 6% strain. This limit corresponds closely with the onset of strain hardening in tensile tests conducted on steel rebar and also on a required minimum strain at fracture for rebar [7]. The determination of the displacement in the barrier was based on the schematic shown in Figure 5.

Figure 5. Schematic of Barrier Displacement.

Engineering strain is defined as the change in length divided by the original length. It represents a stretch. If the strain is prescribe, such as 6% in this case, then the new length, L', drops out of the equation when determining the displacement, Δ. Starting with the mathematical definition of strain in Equation 9, the derivation for the displacement follows in Equations 9 through 12.

$$\varepsilon = \frac{L'-L}{L} = 0.06 \tag{9}$$

$$L' = 1.06 \cdot L \tag{10}$$

12

$$\Delta= \sqrt{\left(\frac{L\prime}{2}\right)^2 + \left(\frac{L}{2}\right)^2} \tag{11}$$

Substituting Equation 10 into Equation 11, the displacement reduces to:

$$\Delta= L\sqrt{0.0309} \tag{12}$$

For now, this definition will suffice until all the components of Equation 7 are defined. The displacement is a function of the effective length of the barrier, which is unknown. However, to finish the strain energy component, Equation 12 must be multiplied by the barriers strength. This strength was a function of the barrier's height, reinforcement, and effective length, again. Hirsch's equation for barrier capacity was substituted into the analysis at this juncture. The force require to induce 6% strain in the rebar was given by Equation 13.

$$F = \frac{8M_b}{L} + \frac{8M_w H}{L} + \frac{M_c L}{H} \tag{13}$$

Where:

F = Force required to induce 6% strain in the barrier, kips

L = Effective length of the barrier, ft

All other terms are as defined earlier. Combining Equations 12 and 13, the strain energy in the barrier for 6% strain in the rebar is given in Equation 14:

$$SE = L\sqrt{0.0309} \left[\frac{8M_b}{L} + \frac{8M_w H}{L} + \frac{M_c L}{H}\right] \tag{14}$$

3.1.3. Conservation of Linear Momentum

When two objects collide in a perfectly plastic manner, they move together with the same velocity. If one of those objects is stationary, it must be accelerated; whereas, the other object must be decelerated. The resulting velocity of the two-object system is equivalent to the impact velocity of the moving object times the ratio of the mass of the moving object and the total mass of the two-object system. This definition of velocity is defined in Equation 15. The two objects were a vehicle and a portion of the barrier. The length of this portion determines the mass that needs to be accelerated. Incidentally, it is also the effective length discussed in the previous section and it replaces the critical length from Hirsch's original YLM.

$$v_f = \frac{m_1}{m_1 + m_2} \cdot v_i \qquad (15)$$

Where:

v_f = Final velocity of the two-object system, ft/s

v_i = Initial velocity of the vehicle, ft/s

m_1 = Mass of the vehicle, lb-ft/s^2 (slugs) = W_T/g

m_2 = Effective mass of the barrier, lb-ft/s^2 (slugs) = $\rho \cdot A \cdot L$

ρ = Density of the concrete barrier = 150 lb/ft^3

A = Cross-sectional area of the concrete barrier, ft^2

Here, again, the effective length, L, was required. Substituting the mass terms for weights, Equation 15 can be rewritten as Equation 16. Note that the constant of gravity drops out of the equation.

$$v_f = \frac{W_T}{W_T + 150 \cdot A \cdot L} \cdot v_i \qquad (16)$$

3.1.4. Conservation of Energy

While accelerating the barrier, the impact zone on the vehicle will crush. This crush is mostly characterized by large-scale plastic deformation and fracture of the steel and plastic in and around the impact zone. All of this damage absorbs energy. The summation of this energy absorption was call the change in internal energy of the vehicle. It was equal to the difference in kinetic energy of the vehicle following the transfer of momentum, as discussed in the previous section. First, the initial and final kinetic energies, by definition, are given in Equations 17 and 18, respectively.

$$KE_i = \frac{W_T}{2g} \cdot v_i^2 \qquad (17)$$

$$KE_f = \frac{W_T}{2g} \cdot v_f^2 \qquad (18)$$

Where:

KE_i = Initial kinetic energy of the vehicle, kip-ft

KE_f = Final kinetic energy of the vehicle, kip-ft

The difference in the initial and final kinetic energy is theoretically equal to the change in the internal energy of the truck. Taking this difference and substituting Equation 16 into Equation 18 results in Equation 19. Note the constant (1/1000) at the end of the equation converts the units from lb-ft to kip-ft.

$$\Delta IE = \frac{W_T}{2g} \cdot v_i^2 \cdot \left[1 - \frac{W_T}{W_T + 150 * A * L}\right] \cdot \frac{1}{1000} \tag{19}$$

3.1.5. Governing Equation

Equation 7 can now be completely assembled. Substituting Equations 8, 14, and 19 into Equation 7 results in Equation 20. For the sake of conciseness, the unit conversion was applied to the strain energy term, placing all three components in units of lb-ft.

$$\frac{W_T}{2g}(v\sin\theta)^2 = 1000 \cdot L\sqrt{0.0309}\left[\frac{8M_b}{L} + \frac{8M_w H}{L} + \frac{M_c L}{H}\right] + \frac{W_T}{2g}v_i^2\left[1 - \frac{W_T}{W_T + 150 * A * L}\right] \tag{20}$$

3.2. Moment Capacities

A critical set of parameters in Equation 20 are the various moment capacities of the barrier. The three moment capacities are: (1) beam, M_b; (2) wall, M_w; and (3) cantilever, M_c. All three were illustrated in Hirsch's diagram, which was reproduced in Figure 4. All three are dependent on the reinforcement size and placement as well as the 28-day compressive strength of the concrete and its cross-sectional dimensions. The yield strength of the rebar and the compressive strength of the concrete were ascertained from the test reports or drawings of bridge rails that are federally accepted for use on the National Highway System. Generally, the rebar was comprised of Grade 60 steel, and the concrete had a compressive strength of between 3.6 and 4.0 ksi. Also, the portion of the concrete place in compressive due to external loading was simplified by the Whitney stress block, which assumes that the compressive block is rectangular in shape. The depth of this block was determined by Equation 21.

$$a = \frac{A_s f_y}{\beta_1 \cdot f_c' \cdot b} \tag{21}$$

Where:

$a =$ Height of the Whitney stress block, inches

$A_s =$ Combined area of tensile steel rebar, in^2

15

f_y = Yield stress of the rebar, ksi

β_1 = Reduction factor between 0.65 and 0.85

f_c' = 28-day compressive strength of concrete, ksi

b = width of the cross section, inches

This stress block defines the compressive side of the concrete, whereas the steel rebar in tension defines the tensile side of the concrete. The two must be equilibrium. Using the distance between the compressive forces (characterized by the midpoint of the stress block), the moment capacity of the beam/wall/cantilever is that distance times the tensile capacity of the rebar. Generally, the nominal moment capacity of a reinforced concrete design is given by Equation 22.

$$M_N = A_s f_y \left(d - \frac{a}{2} \right) \tag{22}$$

Where:

M_n = Nominal moment capacity, kip-inch

d = Distance from the compressive face to the center of tensile reinforcement, inches

Most beam capacities were set to zero unless a distinguishable beam was observed on top of the wall. The depth, d, was generally constant, with a symmetrical design. The flexion of the beam, and the barrier in general, resulted in tension on both sides of the barrier at various stages. At the location of peak displacement, for example, the backside of the barrier was in tension. Because the location of the tensile stress could be on either side, the moment capacity for both faces had to be determined. As aforementioned, for beams, these two values were generally equal or zero.

For the wall capacity, M_w, the effective depth to the tensile steel was often dependent on the vertical location of the rebar. For safety shapes, such as the New Jersey barrier, the impact side of the bridge rail was sloped, resulting in decreasing depths as the height increased. To calculate the wall capacity of these sloped shapes, individual calculations were carried out for each level of rebar, which corresponded to a unique depth, d. Each individual level included the area of one rebar, rather than all of the tensile rebar combined. Once the moment capacity for each level was determined, they were all summed to provide the overall wall moment capacity. This process was carried out for both faces, recognizing the possibility that the effective depths

could be different from some of the longitudinal rebars, especially those in the base portion of the safety shape. For vertical walls or single slopes, this process only needed to be done once since the moment capacities for both faces would be equal if the rebar was equidistant from both faces. Finally, the resulting moment capacity was divided by the wall's height, providing a moment capacity per foot, or units of kip-ft/ft.

The cantilever moment capacity was determined by the interface steel design between the deck overhang and the barrier. Generally, the shear reinforcement, or stirrups, of the barrier extended down into the deck. The effective distance from the compressive side to the tensile steel, a process that was repeated for both faces, was used to calculate the moment capacity. The nominal moment capacity from this calculation was divided by the stirrup spacing to provide a moment capacity per foot of wall, or units of kip-ft/ft.

4. ANALYSIS OF EXISTING CONCRETE BRIDGE RAILS

4.1. *Selected Barriers and Moment Capacities*

In order to install a concrete barrier anywhere on the National Highway System, it must first be approved by the FHWA. Longitudinal barriers require crash testing with various vehicles to ensure proper vehicle redirection and structural adequacy of the barrier. The FHWA maintains a listing of acceptable concrete bridge rails on their website [8]. The heights and rebar design may vary for each, but the general list of bridge rails studied in this report are as follows:

- Vertical Wall
- Single Slope
- F-Shape
- New Jersey Shape

In addition, bridge rails evaluated by Hirsch and crash tested by Bloom and Buth were analyzed with the modified YLM. These barriers included the following [1]:

- T5
- T201
- T202

The hand calculations for each of these barriers are provided in Appendix A. For each set of calculations, the tension face was considered to be on both sides because of the inflection points in the rail displacement. Therefore, calculations were carried out for both sides, distinguishing variations is rebar depth when necessary. Also, a 54-inch New Jersey barrier was designed to provide a minimal level of performance as part of this project. It has not been crash tested. The design itself is not recommended for use at this point. It would require full-scale crash testing and FHWA approval before it could be implemented. The resulting moment capacities for each of the barriers are listed in Table 1.

The T5 barrier was a particularly interesting case study. It was crash tested with a 40,000-lb intercity bus in 1976 [1]. The impact severity of this crash test was between TL-4 and TL-5 of NCHRP 350. AASHTO design loads are provided for each test level, 54 kips for TL-4 and 124 kips for TL-5. Using the impact severities of the bus and the two standard tests, the

18

interpolated design load would be 91.8 kips. The modified YLM calculated a barrier capacity of 92.1 kips, a 0.3% difference. This capacity was calculated without any factors of safety or other conservative adjustments. The outcome of the test was that the initial impact induced cracking at the base of the barrier before the secondary tail-slap impact destroyed the barrier. It could be argued that the initial failure of the barrier lead to its subsequent destruction. What is for sure was that the bus was safely redirected. Therefore, the modified YLM is accurate (it should be noted that Hirsch's original method predicted a maximum load of 91 kips), and the design loads for TL-4 and TL-5 are appropriate.

Table 1. Moment Capacities of Analyzed Barriers

Barrier	Height (inch)	Mb (k-ft)	Mw (k-ft/ft)	Mc (k-ft/ft)	Drawing Reference
Vertical Wall	42	59.66	38.76	13.05	[9]
Single Slope	32	0.00	15.05	31.32	[10]
F-Shape	42	0.00	18.02	21.21	[11]
New Jersey	32	0.00	8.03	11.57	[12]
	36	0.00	7.21	11.57	[13]
	42	0.00	7.47	11.57	[14]
	54	0.00	17.59	12.62	NA
T5	32	4.92	2.25	12.20	[1]
T201	27	3.82	1.32	9.49	[1]
T202	27	20.47	0.00	11.86	[1]

4.2. *Iterative Solution for Effective Length*

The modified YLM uses a different approach to solve for the effective length of the barrier, employing the conservation of momentum and energy to accomplish the calculation. The derived form of the modified YLM was provided in Equation 20. However, in this equation, the effective length, L, was non-linear. In other words, when solving for L, it becomes a function of itself. The only way to solve for this is to essentially guess L on one side of the equation and solve for it on the other side. Then, the process repeats itself, only now instead of guessing L, the previous calculated value is used. This continues until the "guessed" L is reasonably close to the calculated L. Microsoft Excel includes a built-in iterative solver called Goal Seek. Essentially, a cell containing an equation is selected and provided a goal. In this case, the IS cell is selected,

which contains Equation 20, and the goal is set to the IS for the given impact condition. The third and final component of Goal Seek is to determine which cell must be iterative changed. The effective length was allowed to change until the goal for IS was reached. This process is illustrated in Figure 6 through Figure 9. The barrier's capacity, R_w, is highlighted in cell G24. The first figure shows the first "guess" for L and is not accurate. After iteration, L = 12.19995 and IS = 161.230002, or a percent difference of 1.24×10^{-6} %.

	F	G	H
8	20000	161232.6	
9	L (ft)	v_f	Delta KE
10	11.64	19.20256	46624.99
11			
12	I	3.5	
13	Mb	4.92	
14	Mw	2.25	
15	Mc	12.2	
16	H	2.67	
17	IS Goal	161.23	
18	L	8	ft
19	IS	85.05507	
20		66.77232	42.56181
21	Left side	2.734375	*w
22	Right side	47.48181	
23	w	17.36478	kips
24		60.77671	IE Method

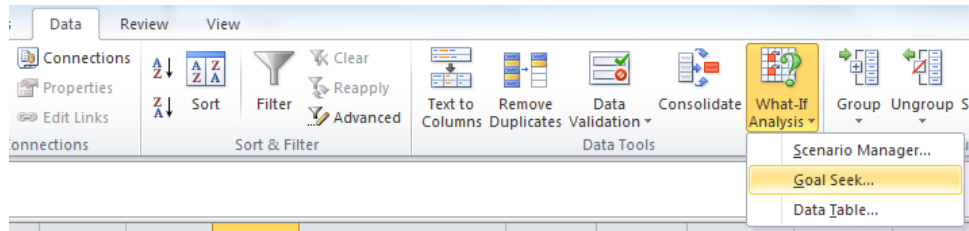Figure 6. Iterative Problem Setup

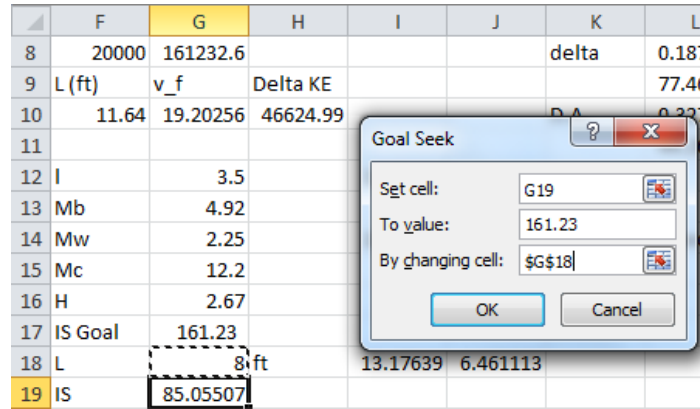Figure 7. Goal Seek Selection

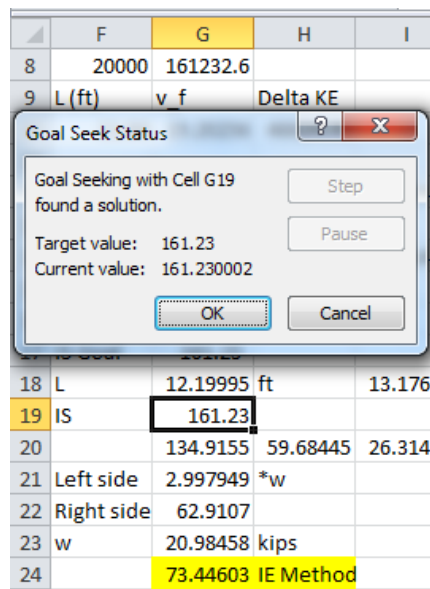Figure 8. Goal Seek Programming

Figure 9. Goal Seek Results

4.3. *Barrier Capacities Based on Modified YLM*

Following the iterative process outlined in the previous section, capacities for barriers approved by the FHWA for use on the National Highway System were calculated and are presented in Table 2. Hirsch's original YLM was used to calculate the resistive capacity (RW) of the barrier for the sake of comparison. The "Vertical Wall" design exhibited the strongest capacity using the traditional YLM; whereas, the 42-inch "New Jersey" barrier exhibited the weakest capacity. Each capacity increased slightly when the conservation of momentum and energy were considered in the modified YLM. Also, capacity decreased as height increased, as demonstrated by the "New Jersey" TL-4 barriers. The increased height adds additional

compliance to the barrier, thus increasing the expected strain energy in the longitudinal rebars. This increase must be offset by reduced loading, which correlates to a reduced capacity.

<p style="text-align:center">Table 2. Summary of Barrier Capacities</p>

Test Level 4					
Barrier	Height (inch)	Mb (k-ft)	Mw (k-ft/ft)	Mc (k-ft/ft)	YLM RW (kips)	Mod. YLM RW (kips)
Vertical Wall	42	59.66	38.76	13.05	166.3	175.6
Single Slope	32	0.00	15.05	31.32	170.6	173.0
F-Shape	42	0.00	18.02	21.21	139.9	148.9
New Jersey	32	0.00	8.03	11.57	71.8	76.3
	36	0.00	7.21	11.57	66.9	69.5
	42	0.00	7.47	11.57	65.4	67.6

Test Level 5					
Barrier	Height (inch)	Mb (k-ft)	Mw (k-ft/ft)	Mc (k-ft/ft)	YLM RW (kips)	Mod. YLM RW (kips)
Vertical Wall	42	59.66	38.76	13.05	185.4	187.4
New Jersey	42	0.00	7.47	11.57	85.3	107.5
	54*	0.00	17.59	12.62	109.7	111.3

Historic Barriers					
Barrier	Height (inch)	Mb (k-ft)	Mw (k-ft/ft)	Mc (k-ft/ft)	YLM RW (kips)	Mod. YLM RW (kips)
T5	32	4.92	2.25	12.2	59.0	92.1
T201	27	3.82	1.32	9.49	48.4	68.7
T202	27	20.47	0	11.86	80.0	55.9

*Steel reinforcement scaled up from 42-inch NJ barrier

The far right component of Equation 20 represents the internal energy of the vehicle during the impact event. As discussed previously, this term was derived by using the conservation of linear momentum to approximate the resulting velocity of the vehicle, which then correlated to a reduced kinetic energy. The magnitude of this reduction was the change in internal energy of the vehicle, which is reported in Table 3 for various barrier designs.

Table 3. Summary of Truck Internal Energy

Test Level	Barrier	Height (inch)	Modified YLM		
			ΔIE_T (k-ft)	IS (k-ft)	%(ΔIE_T)
TL-4	Vertical Wall	42	39.9	150.17	26.6%
	Single Slope	32	16.5	150.17	11.0%
	F-Shape	34	21.2	150.17	14.1%
	New Jersey	32	20.5	150.17	13.7%
		36	20.2	150.17	13.4%
		42	22.2	150.17	14.8%
		54	11.6	150.17	7.7%
TL-5	Vertical Wall	42	52.6	447.87	11.8%
	New Jersey	42	46.9	447.87	10.5%
		54*	43.7	447.87	9.8%

*Steel reinforcement scaled up from 42-inch NJ barrier

5. ENERGY VERIFICATION VIA LS-DYNA

5.1. *Introduction*

LS-DYNA is a computer program that is capable of solving complex, non-linear equations. The present research is an ideal candidate for using this software. The energy dissipation of the vehicle alone is a complex summation of the deformation and forces for hundreds of components, each acting together through various modes of contact. Adding to the complexity, the vehicle must interact with the barrier, transferring energy over a distributed area. The culminating point is that the impact between a vehicle and a barrier is highly non-linear. Even the analytical calculations described previously in this report required iteration to solve a non-linear equation. LS-DYNA is also proficient with explicit time step calculations. Explicit time steps are a function of the size of the mesh used by LS-DYNA in the finite element analysis. The speed of sound through each material type is also considered. Explicit time steps create small enough increments in time that each element has a chance to capture stress waves propagating through the material. This is only required for dynamic impact conditions, such as a vehicle striking bridge rail. As such, a preliminary LS-DYNA model was created and simulated to verify energy dissipation in the vehicle. Knowing the initial kinetic energy and the vehicle, if the internal energy of the vehicle is accurate, then the strain energy in the barrier must also be accurate.

To accomplish this verification, a material model for the concrete was calibrated using dynamic impact test results. These tests were conducted at the Barber Laboratory for Advanced Safety Education and Research (BLASER) in Leeds, Alabama. Reinforced concrete beams were dynamically tested in 3-point bending.

Next, an LS-DYNA model was created to replicate the impact conditions for the beam testing. A material type (*MAT_159) was assigned to the concrete in the beam, and a steel material model with yielding (*MAT_003) was assigned to the rebar. The damage coefficient in the concrete model was calibrated until the simulation results matched the test results.

Finally, the calibrated material model for concrete was substituted into a New Jersey barrier model, which was then impacted by a single-unit truck model created by the National Crash Analysis Center (NCAC) [15]. Because this was only a preliminary model, rather than a

full-scale modeling endeavor, only one impact condition for a single barrier type was analyzed. The results were processed by comparing the summation of the internal energies of all truck parts to the expected internal energy component of the spreadsheet calculations from the previous chapter.

5.2. *Concrete Beam Testing*

Six reinforced concrete beams were constructed and dynamically tested at the BLASER facility. Each beam was 10 feet long with a square cross section of 12 inches per side. Steel stirrups were placed in the beams to provide shear reinforcement, ensuring failure in tension due to bending. Longitudinal rebars were placed on the tension side of the beam to resist this bending, with an effective depth to the center of the rebar of 10 inches. Six beams were tested, two per design. The designs were varied by rebar size (either No. 4 or No. 6) and the 28-day compressive strength, f_c' (either 4,000 or 6,000 psi). Conceptually, the "baseline" beam used No. 4 bars with a compressive strength of 4,000 psi. Design 2 changed the rebar to No. 6 but kept the same compressive strength. Design 3 used the baseline rebar but 6,000-psi compressive strength. Note that the fourth possible design, No. 6 bars with 6,000-psi concrete, was not tested.

The BLASER facility includes a large concrete pad measuring approximately 150 ft by 300 ft. At one end, a 4-ft tall bogey block measuring 8 ft per side was constructed as part of the construction of this facility. Effectively, this block represents a rigid backstop. Two steel fixtures were constructed to attach to the bogey block and suspend the concrete beam at a height amicable with the bogey vehicle. This bogey vehicle was steel frame partially filled with concrete and included four tires. It weighs 4,250 lbs. It was towed with a reverse cable system, and it was guided by setting tires from one side in a grove formed by W-beam guardrail segments lain on the ground. This test setup is shown in Figure 10 and Figure 11.

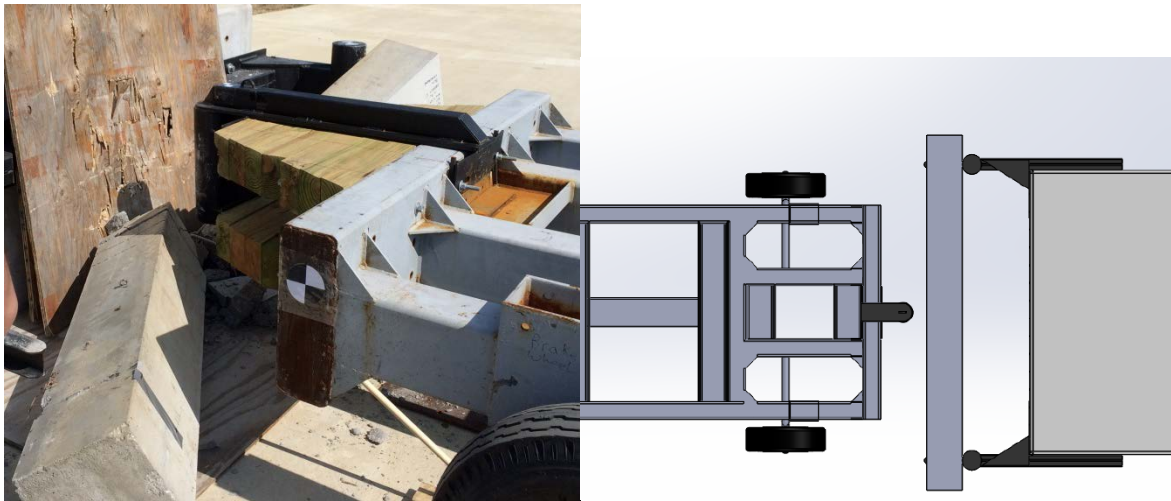**Figure 10. Beam Test Setup with Speed Dowels and Track Guidance**

Figure 11. Bogey Impact Head and Orientation

The bogey vehicle was instrumented with accelerometers to measure the forces exerted on the beam by the impactor. Also, the supports holding up the beam were spaced 8 ft 4 in. apart from each other and represented two rolling supports, resulting in only two reaction forces. Using the mass of the bogey vehicle, the force it exerted on the beam was calculated according to Newton's 2nd law: $F = ma$. Then, the applied moment carried by the beam was calculated according to Equation 23.

$$M = \frac{FL}{2} \qquad (23)$$

Where:

    M = Moment applied by the force, F

F = Force applied by the bogey vehicle

L = Length between supports, = 8 ft 4 in.

The moment capacities determined by physical testing, using the accelerometers, were compared with the hand calculated moment capacities based on the cross section of the beam. This comparison was made only to verify the accuracy of the accelerometer data. These calculated moment capacities were determined using Equation 21 and 22. The resulting calculations are shown in Table 3.

Table 4. Expected Moment Capacities for Beam Designs

Parameter	Design 1	Design 2	Design 3
f_y (psi)	60,000	60,000	60,000
f_c' (psi)	4,000	4,000	6,000
A_s (in^2)	0.8	1.76	0.8
b (in)	12	12	12
d (in)	10	10	10
β_1	0.85	0.85	0.75
a (in)	1.18	2.59	0.89
M_N (k-ft)	37.65	76.61	38.22

5.3. *Material Model*

The beams were simulated in order to validate the concrete material model by calibrating the damage to the model until it matched the physical crash tests. The supports and the impactor were simplified in the model as rigid cylinders with diameters equal to the physical test setup. The mass density of the impactor cylinder was modified such that the cylinder's final mass matched the physical bogey vehicle. Each of the six crash tests were replicated with LS-DYNA by modifying the impact speed according to the speed observed in the crash tests.

The beam itself was meshed with solid and discrete elements. It was comprised of two materials: concrete (solid elements) and steel (beam elements). In total, the model, including the impactor, had 404,259 elements and 427,800 nodes. The solid elements were controlled by a fully integrated element formulation (ELFORM = 3). The beam elements were controlled by the resultant truss element formulation (ELFORM = 3). Each rebar was represented by a string of discrete beam elements, with the start and end node of each beam correlating to two nodes of the

solid concrete elements. This required composite action between the concrete and the rebar, which was a reasonable expectation unless the concrete spalled. At which point, in the model, the solid elements would erode away, but the steel beam elements would remain until their failure strain was reach, which was defined in the material card.

The material model in LS-DYNA that was chosen for steel was the plastic, kinematic model (also known as *MAT_003). This material model takes as input Young's modulus, Poisson's ratio, yield stress, tangent modulus, and strain at failure. The tested beams utilized Grade 60 rebar, which has a nominal yield stress of 60 ksi. Up until this point, the stress-strain curve is linearly elastic with a slope defined by Young's modulus. After this point, it is still linear, but it now has a slope defined by the tangent modulus, and all strain occurring after this yield point is considered permanent. A screen shot of the material model used throughout this preliminary model for steel rebar is shown in Figure 12. Note that the following materials are assigned metric values, using units of kg, ms, MPa, and mm.

```
*MAT_PLASTIC_KINEMATIC_TITLE
Steel
$#     mid          ro          e          pr        sigy        etan        beta
        4 7.8300E-9 2.0700E+5  0.300000 532.41302 1107.7280      0.000
$#     src         srp         fs          vp
     0.000       0.000   0.114000       0.000
```

Figure 12. Steel Rebar Material Card

The material model in LS-DYNA that was chosen for concrete was, conveniently, the concrete model (also known as *MAT_159_CONCRETE). This specific version includes hidden default parameters that cannot be changed unless the more general concrete model (*MAT_159) is used. With this preconfigured material model, the only three parameters are the damage coefficient, the compressive strength, and the average aggregate size. The average aggregate size was set to ¾ in. for all models. The compressive strength was modified depending on which of the three designs was being modeled. The damage coefficient was adjusted to obtain consistency between the model and the physical tests. This adjustment was the tool used to calibrate the concrete material model. After trial and error, this damage coefficient was set to 1.05 for all beam and barrier models. A screen shot of the concrete material model is shown in Figure 13.

```
*MAT_CSCM_CONCRETE_TITLE
Concrete
$#     mid           ro      nplot       incre       irate       erode       recov     itretrc
         2   2.6490E-9          1       0.000           0    1.050000   10.000000           0
$#    pred
       0.000
$#     fpc         dagg       units
 27.579000   19.000000           2
```

Figure 13. Concrete Material Card

These two material models, and specifically the damage coefficient for the concrete model, provided reasonably accurate fracture patterns in the simulated beam impact. Also, the force-deflection curves were compared, and it was determined that the model provided reasonable solutions for the three designs. An overhead view of the physical and virtual beams for Design 3 is shown in Figure 14.
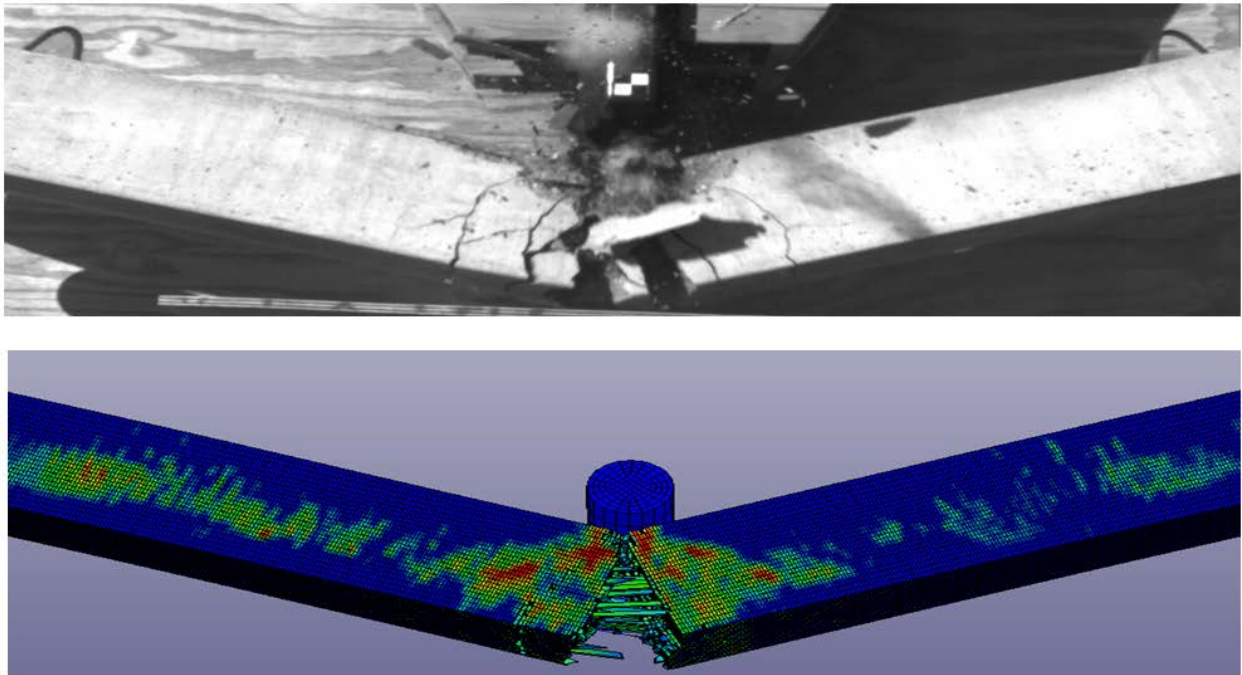
Figure 14. Design 3 Comparisons

The physical beams were impacted with the intent to fracture them, exceeding their capacities. This allowed researchers to analyze the beams' behaviors through the entire range of strength. However, as can be noted in the models, many of the concrete elements became highly distorted near the end of the simulation, at large displacements. Normally, this would be a concern that should be rectified in order to create a robust material model. However, because this

was part of a preliminary comparison, and because the modified YLM was only concerned with strains in the rebar of 6% or less, the material model behavior for larger strains was not investigated further.

5.4. *Internal Energy of Truck*

The steel and concrete material models previously referenced were considered accurate for small to moderate strains, including the 6-percent strain limit imposed in the modified YLM. Therefore, the modeling effort proceeded by inserting these two material models into a full-scale crash model involving a New Jersey bridge rail and an NCHRP 350 TL-4 vehicle (a single-unit truck). The barrier model had 9 parts, 338,462 elements, and 345,519 nodes. The truck model was downloaded from the NCAC model archive website [15]. It included 151 parts, 35,400 elements, and 38,949 nodes. It was given an initial velocity of 49.7 mph, and the bridge rail was oriented such that the impact angle of the truck was 15 degrees. Other than initial conditions, the truck model was unmodified, and details of the model can be found on the referenced website. A screen shot of the orientation of the model is shown in Figure 15.
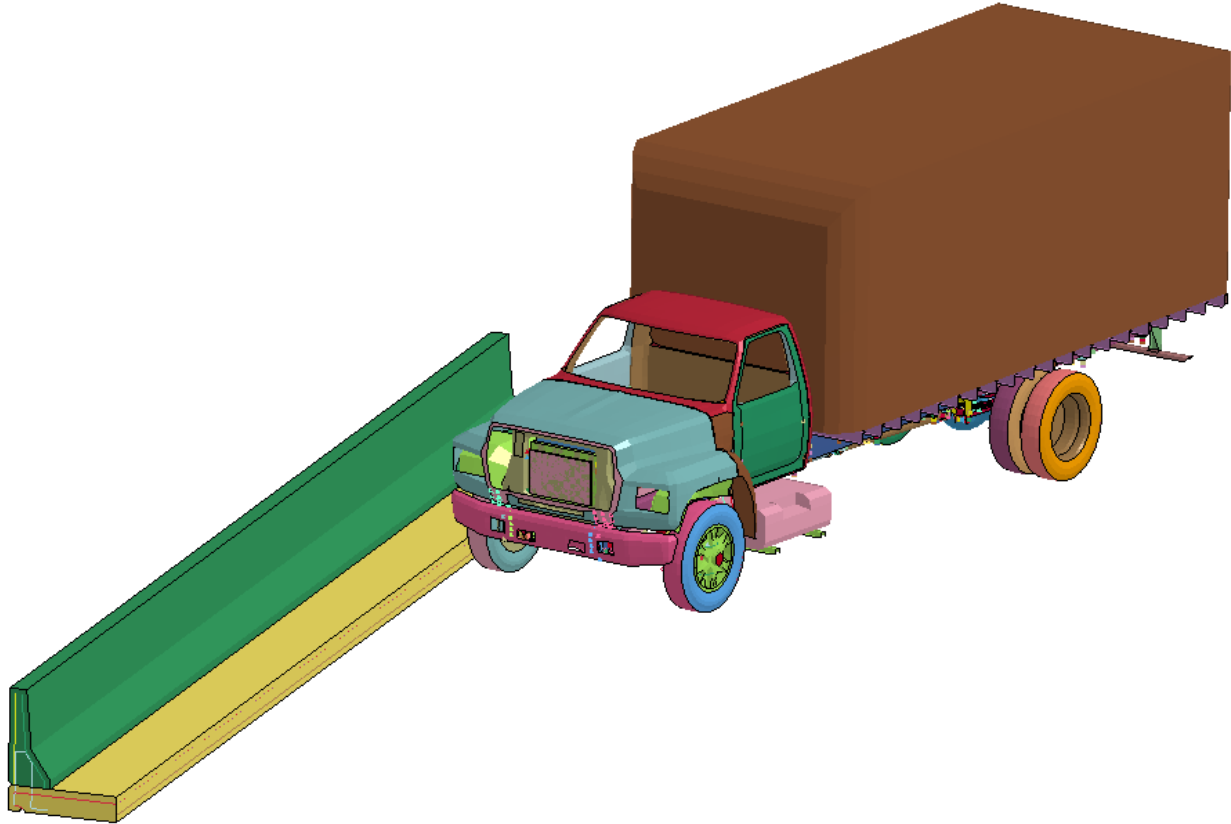
The New Jersey bridge rail was modeled in a similar fashion as the concrete beams. Concrete was discretized by solid elements, and rebar was discretized by discrete beam elements that shared nodes with the concrete. A bridge deck overhang was also included. Steel stirrup from the bridge rail extended down into the deck overhang, providing a connection between the two concrete components. The total width of the modeled deck overhang was 39 inches, and the remainder of the virtual bridge deck was modeled with a planar rigid wall in order to keep the truck at deck level prior to impact. The element formulation and material cards were the same as the beam model described in the previous section.

Energy calculations were the primary interest in the post processing of the model, however barrier deflection, specifically in the rebar, was requisite for comparison to the modified YLM. The deflections in the longitudinal rebar were tracked and used to calculate strains. When the maximum rebar strain reached 6%, that time was flagged as t'. At t', the energy levels were investigated. Particularly, the internal energy due to the deformation of the vehicle was investigated. The LS-PrePost post-processor was used to calculate this energy. Unfortunately, the

31

total internal energy of the truck was not a trivial number to report. Global calculations were available through the GLSTAT ASCII file output, but this includes the internal energy of the barrier system as well. Therefore, internal energies of selected parts were added together using the ASCII file output from the MATSUM option in LS-DYNA. The total vehicle internal energy was 17.9 kip-ft (11.9% or the impact severity, or IS). In contrast, the calculated internal energy of the vehicle using the modified YLM was 20.5 kJ (13.7% of the IS).

6. DISCUSSION OF RESULTS

Deformation in the barrier and overhang system is an integral part in the crash event. Generally, the specific deformation, and by extension energy absorption, of the barrier and overhang system are not considered. Instead, it is assumed that the barrier is rigid, and that the absorbed energy needed to redirect the vehicle is absorbed entirely by the vehicle. The modified YLM was developed under the assumption that the momentum transfer between the vehicle and the barrier/deck system was significant. Computer simulations support this belief when the barrier and deck were modeled with deformable materials, rather than as rigid objects.

The ramification of this extra energy absorption is that the critical impact load imparted on the barrier is reduced. The deformation of the wall also elicits an extended period of attenuation of the vehicle's velocity. Force can be tied to mass and velocity by way of the impulse of the impact, which includes a consideration of the duration of the impact event. For short-duration impacts, the force can be high, but if the duration is extended, the forces can be lowered. A compliant barrier will have a longer duration of impact than a perfectly rigid barrier, and as such, the expected loads imparted on the barrier from the vehicle will be lower if the barrier is allowed to deform.

Barrier height also effects barrier compliance, and ultimately the load applied to the barrier. The effect of barrier height is multi-faceted, but if the reinforcement design is constant between two different height, the taller barrier will experience less load, including the barrier-deck interface. The taller height creates a longer moment arm, which makes the barrier wall weaker, allowing for more deformation and extending the impact event over a longer period. All of this results in a lower transfer of load from the truck to the barrier. It also means that taller barriers have less resistive capacity unless they are given more reinforcement than their shorter counterparts. In general, a taller barrier is designed with more steel reinforcement since the application of taller barriers generally coincides with larger vehicles. They are also more susceptible to impacts with the cargo bed of the truck in secondary impacts, which may contribute to the overall damage to the barrier. Tall barriers also help prevent vehicles from rolling over the barrier. This does not necessarily contribute to the energy argument, but it an important consideration when dealing with bridges.

Recent research has recommended increasing the AASHTO transverse design loads up to 93 kips for tall TL-4 barriers and either 160 kips or 260 kips to short or tall TL-5 barriers. These elevated recommendations were likely due to the presence of the secondary impact, known generally as tail slap. In particular, the cargo beds of the TL-4 and TL-5 vehicles made contact with the top of the taller barriers in the computer simulations. However, in the experience of the research team for the current project, this contact between the cargo bed and the top of a 36-inch barrier does not occur. The distance from the ground to the top of the frame of the cargo bed is typically 45 to 50 inches for a TL-4 test vehicle. A schematic of the dimensional drawing for a TL-4 is shown in Figure 16, where the top of the frame of the cargo bed is labeled "l" on the far right.
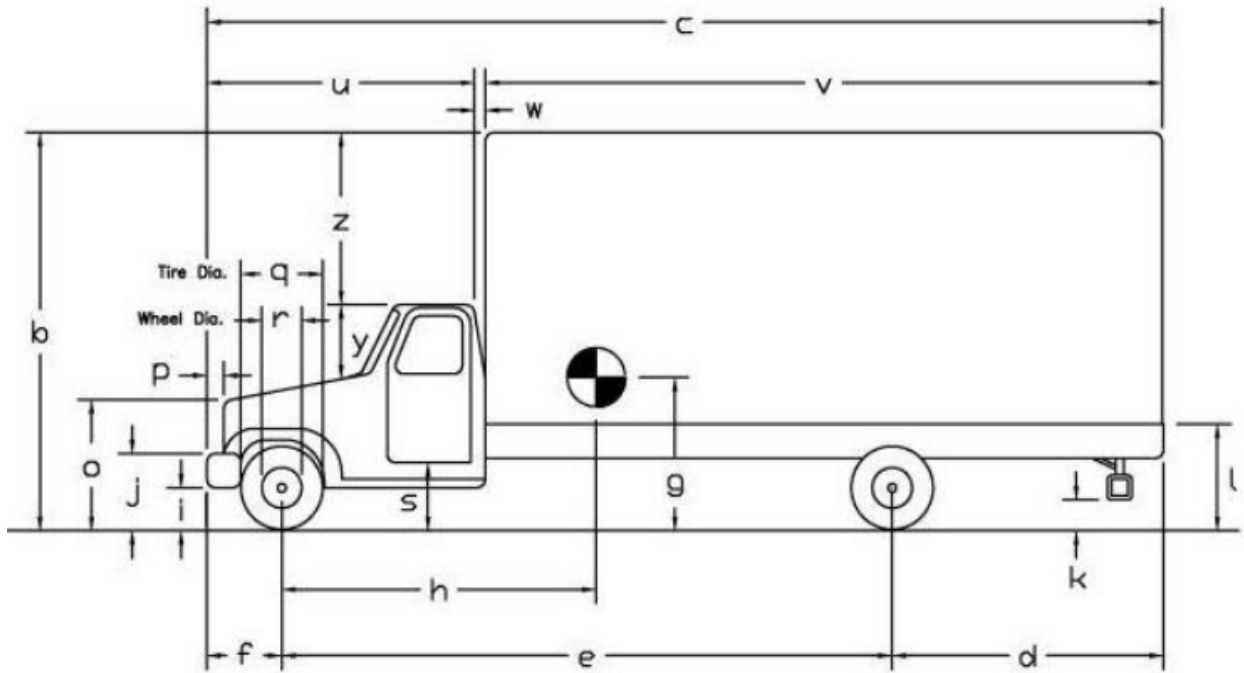
Figure 16. TL-4 Test Vehicle Dimensional Drawing

7. CONCLUSIONS AND RECOMMENDATIONS

The primary focus of the performance of concrete barriers has always been on the vehicle dynamics after the impact. As such, a tendency in the modeling sector has been to establish the shape of barrier and define it as a rigid object. This assists with reducing computational demands from large models. However, it may not be an appropriate assumption for bridge rails, which use less material through the cross section, such as with the New Jersey barrier. It is also install on bridge overhang decks. The net result of these differences relative to standard median barriers is a more compliant system. Since the system has mass, and is allowed to deform, it must, by definition, absorb energy while undergoing this deformation. With a rigid assumption, this absorbed energy is neglected.

During an impact, only a portion of the bridge rail moves, rather than the entire rail. Nevertheless, because a portion of the rail moves after impact, the law of the conservation of momentum applies. This law dictates that the masses of two separate objects traveling at different speeds combine to move at the same speed. The mass of the bridge rail is determined by what portion of the bridge rail moves. However, this determination is not trivial and requires determining an effective length.

The modified YLM accounted for momentum transfer of the vehicle to a portion of the barrier, and it included a consideration for the deformation of the barrier itself. With all of these considerations, all FHWA-approved bridge rails for TL-4 and TL-5 were adequate when compared to AASHTO's current design transverse load of 54 kips. None of the crash tested bridge rails experience significant damage at the base or through the height of the system.

The design loads corresponding to TL-4 and TL-5 have been the subject of debate lately with the implementation of MASH as a replacement for NCHRP 350. The only difference in the two for TL-4 was additional mass for the truck. TL-5 was not changed in any way. Recent research has suggested that the AASHTO transverse design loads should be increased to as high as 93 kips and 260 kips for TL-4 and TL-5, respectively, depending on the height of the barrier. These numbers were based on complex computer simulations. However, the traditional YLM was modified to included momentum transfer and barrier deformation, resulting in a less demanding set of computations without sacrificing accuracy. With this modified YLM, a

historical bridge rail, crash tested in 1976, was evaluated because it exhibited structural failure but still redirected the bus. This suggests that the barrier was very near its limit and capacity to redirect the bus. Interpolating the impact severity between the TL-4 and TL-5 levels, the interpolated design load (between 54 and 124 kips) would have been 91.8 kips. The capacity according to the modified YLM was 92.1 kips, a 0.3% difference. This correlation suggests that the modified YLM is accurate and that the AASHTO design loads, 54 and 124 kips, are appropriate.

8. REFERENCES

1. Hirsch

2. AASHTO Bridge Specifications

3. NCHRP 350

4. MASH

5. TTI design loads

6. NCHRP 86

7. Steel rebar reference

8. FHWA website

9. Vertical Wall: http://guides.roadsafellc.com/Documents/SBC01d/Drawings/1993GSBH.pdf; accessed: 12/18/2015.

10. Single Slope: http://safety.fhwa.dot.gov/roadway_dept/policy_guide/road_hardware/barriers/bridgerailings/docs/appendixb7g.pdf; accessed: 12/18/15

11. F-Shape: http://safety.fhwa.dot.gov/roadway_dept/policy_guide/road_hardware/barriers/bridgerailings/docs/appendixb7g.pdf; accessed: 12/18/15

12. NJ 32 – TTI Report

13. NJ 36 ref

14. NJ 42 ref

15. NCAC website

9. APPENDICES

A. Barrier Moment Capacity Calculations

1. Vertical Wall

Given:

$$f_y = 60 \; ksi \tag{A.1.1}$$

$$f_c' = 3.6 \; ksi \tag{A.1.2}$$

Rebar size: #8 (A.1.3)

$$A_s = 0.79 \; in^2 \; per \; bar \tag{A.1.4}$$

Beam width: $b = 8.86 \; in$ (A.1.5)

Beam depth: $D_b = 12 \; in$ (A.1.6)

Cover: $d_c = 1.5748 \; in$ (A.1.7)

Bars in beam: $n_b = 2$ (A.1.8)

Bars in wall: $n_w = 4$ (A.1.9)

Wall height: $h = 33.27 \; in$ (A.1.10)

Wall depth: $D_w = 10.43 \; in$ (A.1.11)

Stirrup size: #5 (A.1.12)

Stirrup spacing: $s = 11.811 \; in$ (A.1.13)

Beam Moment:

$$a = \frac{n_b A_s f_y}{\beta_1 f_c' b} = \frac{(2)(0.79)(60)}{(0.85)(3.6)(8.86)} = 3.4967 \; in \tag{A.1.14}$$

$$d_b = D_b - d_c - {}^5\!/_8 - 0.5\left({}^8\!/_8\right) = 9.3 \; in \tag{A.1.15}$$

$$M_N = n_b A_s f_y \left(d_b - \frac{a}{2}\right) = (2)(0.79)(60)\left(9.3 - \frac{3.4967}{2}\right) = 715.92 \; kip - in \tag{A.1.16}$$

$$M_b = \frac{M_N}{12} = 59.66 \; kip - ft \tag{A.1.17}$$

Wall Moment:

$$a = \frac{n_b A_s f_y}{\beta_1 f_c' b} = \frac{(4)(0.79)(60)}{(0.85)(3.6)(33.27)} = 1.86236 \; in \tag{A.1.18}$$

$$d_w = D_w - d_c - {}^5\!/_8 - 0.5\left({}^8\!/_8\right) = 7.7 \; in \tag{A.1.19}$$

$$M_N = n_b A_s f_y \left(d - \frac{a}{2}\right) = (4)(0.79)(60)\left(7.7 - \frac{1.86236}{2}\right) = 1{,}289.68 \; kip - in \tag{A.1.20}$$

$$M_w = \frac{M_N}{h} = 38.76 \; \frac{kip - ft}{ft} \tag{A.1.21}$$

Cantilever Moment:

$$a = \frac{n_b A_s f_y}{\beta_1 f_c' b} = \frac{(1)(0.31)(60)}{(0.85)(3.6)(11.811)} = 0.514642 \ in \qquad (A.1.22)$$

$$d_c = D_w - d_c - 0.5\left(\frac{5}{8}\right) = 8.55 \ in \qquad (A.1.23)$$

$$M_N = A_s f_y \left(d - \frac{a}{2}\right) = (0.31)(60)\left(8.55 - \frac{0.514642}{2}\right) = 154.17 \ kip - in \qquad (A.1.24)$$

$$M_w = \frac{M_N}{s} = 13.05 \ \frac{kip-ft}{ft} \qquad (A.1.25)$$

2. Single Slope

Given:

$$f_y = 60 \ ksi \qquad (A.2.1)$$

$$f_c' = 4.0 \ ksi \qquad (A.2.2)$$

Rebar size: #4 $\qquad$ (A.2.3)

$$A_s = 0.20 \ in^2 \ per \ bar \qquad (A.2.4)$$

Top width: $b_t = 9.5 \ in$ $\qquad$ (A.2.5)

Bottom width: $b_b = 15.675 \ in$ $\qquad$ (A.2.6)

Cover: $d_c = 1.5 \ in$ $\qquad$ (A.2.7)

Bars in wall: $n_w = 4$ $\qquad$ (A.2.8)

Wall height: $h = 32 \ in$ $\qquad$ (A.2.9)

Stirrup size: #5 $\qquad$ (A.2.10)

Stirrup spacing: $s = 8 \ in$ $\qquad$ (A.2.11)

Slope of face: $\alpha = 10.8 \ degrees$ $\qquad$ (A.2.12)

Beam Moment:

$$M_b = 0 \ kip - ft \qquad (A.2.13)$$

Wall Moment:

$$a = \frac{n_b A_s f_y}{\beta_1 f_c' b} = \frac{(4)(0.20)(60)}{(0.85)(4.0)(32)} = 0.415225 \ in \qquad (A.2.14)$$

$$D_1 = b_t - h_1 \tan 10.8 = 9.5 + (1.75)(0.19076) = 9.83383 \ in \qquad (A.2.15)$$

$$D_2 = b_t - h_2 \tan 10.8 = 9.5 + (9.5)(0.19076) = 11.3122 \ in \qquad (A.2.16)$$

$$D_3 = b_t - h_3 \tan 10.8 = 9.5 + (17.25)(0.19076) = 12.7906 \ in \tag{A.2.17}$$

$$D_4 = b_t - h_4 \tan 10.8 = 9.5 + (25)(0.19076) = 14.269 \ in \tag{A.2.18}$$

$$d_{avg} = \frac{\sum(D_i - 1.5 - 0.5 \cdot 0.625)}{4} = 10.2389 \ in \tag{A.2.19}$$

$$M_N = n_w A_s f_y \left(d - \frac{a}{2}\right) = (4)(0.20)(60)\left(10.2389 - \frac{0.415225}{2}\right) = 481.502 \ k-in \tag{A.2.20}$$

$$M_w = \frac{M_N}{h} = 15.05 \ \frac{kip-ft}{ft} \tag{A.2.21}$$

Cantilever Moment:

$$a = \frac{n_b A_s f_y}{\beta_1 f_c' b} = \frac{(1)(0.31)(60)}{(0.85)(4.0)(8)} = 0.683824 \ in \tag{A.2.22}$$

$$d_c = b_b - d_c - 0.5\left(\frac{5}{8}\right) = 13.8125 \ in \tag{A.2.23}$$

$$M_N = A_s f_y \left(d - \frac{a}{2}\right) = (0.31)(60)\left(13.8125 - \frac{0.683824}{2}\right) = 250.553 \ k-in \tag{A.2.24}$$

$$M_c = \frac{M_N}{s} = 31.32 \ \frac{kip-ft}{ft} \tag{A.2.25}$$

3.   F-Shape

<u>Given:</u>

$$f_y = 40 \ ksi \tag{A.3.1}$$

$$f_c' = 3.6 \ ksi \tag{A.3.2}$$

Rebar size: #7 (A.3.3)

$$A_s = 0.60 \ in^2 \ per \ bar \tag{A.3.4}$$

Top width: $b_t = 9.0 \ in$ (A.3.5)

Bottom width: $b_b = 17.25 \ in$ (A.3.6)

Cover: $d_c = 1.5 \ in$ (A.3.7)

Bars in wall: $n_w = 4$ (A.3.8)

Wall height: $h = 42 \ in$ (A.3.9)

Stirrup size: #5 (A.3.10)

Stirrup clearance: $d_s = 3 \ in$ (A.3.11)

Stirrup spacing: $s = 8 \ in$ (A.3.12)

Slope of face: $\alpha = 6.02066 \ degrees$ (A.3.13)

<u>Beam Moment:</u>

$$M_b = 0 \ kip - ft \tag{A.3.14}$$

<u>Wall Moment:</u>

$$a = \frac{n_b A_s f_y}{\beta_1 f_c' b} = \frac{(4)(0.60)(40)}{(0.85)(3.6)(42)} = 0.746965 \ in \tag{A.3.15}$$

$$D_1 = b_t + h_1 \tan 6.02 = 9.0 + (3)(0.105469) = 9.31641 \ in \tag{A.3.16}$$

$$D_2 = b_t + h_2 \tan 6.02 = 9.0 + (12)(0.105469) = 10.2656 \ in \tag{A.3.17}$$

$$D_3 = b_t + h_3 \tan 6.02 = 9.0 + (22)(0.105469) - 1.5 = 9.82031 \ in \tag{A.3.18}$$

$$D_4 = b_t + h_4 \tan 6.02 = 9.0 + (32)(0.105469) - 1.5 = 10.875 \ in \tag{A.3.19}$$

$$d_{avg} = \frac{\Sigma(D_i - 1.5 - 0.5 \cdot 0.625)}{4} = 8.25683 \ in \tag{A.3.20}$$

$$M_N = n_w A_s f_y \left(d - \frac{a}{2}\right) = (4)(0.60)(40)\left(8.25683 - \frac{0.746965}{2}\right) = 756.801 \ k - in \tag{A.3.21}$$

$$M_w = \frac{M_N}{h} = 18.02 \ \frac{kip - ft}{ft} \tag{A.3.22}$$

Cantilever Moment:

$$a = \frac{n_b A_s f_y}{\beta_1 f_c' b} = \frac{(1)(0.31)(40)}{(0.85)(3.6)(8)} = 0.506536\ in \tag{A.3.23}$$

$$d_c = b_b - d_s - 0.5\left(\frac{5}{8}\right) = 13.9375\ in \tag{A.3.24}$$

$$M_N = A_s f_y\left(d - \frac{a}{2}\right) = (0.31)(40)\left(13.9375 - \frac{0.506536}{2}\right) = 169.684\ k - in \tag{A.3.25}$$

$$M_c = \frac{M_N}{s} = 21.21\ \frac{kip-ft}{ft} \tag{A.3.26}$$

4. New Jersey Shape – 32"

<u>Given:</u>

$f_y = 60\ ksi$ (A.4.1)

$f_c' = 3.6\ ksi$ (A.4.2)

Rebar size: #4 (A.4.3)

$A_s = 0.20\ in^2\ per\ bar$ (A.4.4)

Top width: $b_t = 6.0\ in$ (A.4.5)

Bottom width: $b_b = 15\ in$ (A.4.6)

Cover: $d_c = 1.5\ in$ (A.4.7)

Bars in wall: $n_w = 4$ (A.4.8)

Wall height: $h = 32\ in$ (A.4.9)

Stirrup size: #5 (A.4.10)

Stirrup clearance: $d_s = 3\ in$ (A.4.11)

Stirrup spacing: $s = 8\ in$ (A.4.12)

Slope of top face: $\alpha = 6.00901\ degrees$ (A.4.13)

Slope of bottom face: $\gamma = 34.992\ degrees$ (A.4.14)

<u>Beam Moment:</u>

$M_b = 0\ kip - ft$ (A.4.15)

<u>Wall Moment:</u>

$a = \dfrac{n_b A_s f_y}{\beta_1 f_c' b} = \dfrac{(4)(0.20)(60)}{(0.85)(3.6)(32)} = 0.490196\ in$ (A.4.16)

Backside

$d_1 = b_t + (2)\tan 6.01 - 1.8125 = 4.37171\ in$ (A.4.17)

$d_2 = b_t + (10)\tan 6.01 - 1.8125 = 5.1875\ in$ (A.4.18)

$d_3 = b_t + (18)\tan 6.01 - 1.8125 = 6.00329\ in$ (A.4.19)

$d_4 = b_t + (26)\tan 6.01 - 1.8125 = 8.7373\ in$ (A.4.20)

$M_1 = A_s f_y \left(d_1 - \dfrac{a}{2}\right) = (0.20)(60)\left(4.37171 - \dfrac{0.490196}{2}\right) = 49.52\ k - in$ (A.4.21)

$M_2 = A_s f_y \left(d_2 - \dfrac{a}{2}\right) = (0.20)(60)\left(5.1875 - \dfrac{0.490196}{2}\right) = 59.31\ k - in$ (A.4.22)

$$M_3 = A_s f_y \left(d_3 - \frac{a}{2}\right) = (0.20)(60)\left(6.00329 - \frac{0.490196}{2}\right) = 69.10 \ k-in \tag{A.4.23}$$

$$M_4 = A_s f_y \left(d_4 - \frac{a}{2}\right) = (0.20)(60)\left(8.2875 - \frac{0.490196}{2}\right) = 101.91 \ k-in \tag{A.4.24}$$

$$M_N = \sum M_i = 279.83 \ kip-in \tag{A.4.25}$$

Frontside

$$d_1 = b_t + h_1 \tan 6.01 - 1.8125 = 4.37171 \ in \tag{A.4.26}$$

$$d_2 = b_t + h_2 \tan 6.01 - 1.8125 = 5.1875 \ in \tag{A.4.27}$$

$$d_3 = b_t + h_3 \tan 6.01 - 1.8125 = 6.00329 \ in \tag{A.4.28}$$

$$d_4 = \left(\frac{d_3 - d_1}{15.5}\right)(7.75) + d_3 = 6.81908 \ in \tag{A.4.29}$$

$$M_1 = A_s f_y \left(d_1 - \frac{a}{2}\right) = (0.20)(60)\left(4.37171 - \frac{0.490196}{2}\right) = 49.52 \ k-in \tag{A.4.30}$$

$$M_2 = A_s f_y \left(d_2 - \frac{a}{2}\right) = (0.20)(60)\left(5.1875 - \frac{0.490196}{2}\right) = 59.31 \ k-in \tag{A.4.31}$$

$$M_3 = A_s f_y \left(d_3 - \frac{a}{2}\right) = (0.20)(60)\left(6.00329 - \frac{0.490196}{2}\right) = 69.10 \ k-in \tag{A.4.32}$$

$$M_4 = A_s f_y \left(d_4 - \frac{a}{2}\right) = (0.20)(60)\left(6.81908 - \frac{0.490196}{2}\right) = 78.89 \ k-in \tag{A.4.33}$$

$$M_N = \sum M_i = 256.81 \ kip-in \tag{A.4.34}$$

$$M_w = \frac{\min M_N}{h} = \frac{256.81}{32} = 8.03 \ \frac{kip-ft}{ft} \tag{A.4.35}$$

Cantilever Moment:

$$a = \frac{n_b A_s f_y}{\beta_1 f_c' b} = \frac{(1)(0.31)(60)}{(0.85)(3.6)(8)} = 0.759804 \ in \tag{A.4.36}$$

Bottom Section

$$d_c = 15 - 2.86 = 11.2378 \ in \tag{A.4.37}$$

$$M_N = A_s f_y \left(d - \frac{a}{2}\right) = (0.31)(60)\left(11.2378 - \frac{0.759804}{2}\right) = 201.96 \ k-in \tag{A.4.38}$$

Top Section

$$d_c = 5.35598 \ in \tag{A.4.39}$$

$$M_N = A_s f_y \left(d - \frac{a}{2}\right) = (0.31)(60)\left(5.35598 - \frac{0.759804}{2}\right) = 92.56 \ k-in \tag{A.4.40}$$

$$M_c = \frac{\min M_N}{s} = \frac{92.56}{8} = 11.57 \ \frac{kip-ft}{ft} \tag{A.4.41}$$

Given:

$f_y = 60 \; ksi$ $\qquad$ (A.5.1)

$f_c' = 3.6 \; ksi$ $\qquad$ (A.5.2)

Rebar size: #4 $\qquad$ (A.5.3)

$A_s = 0.20 \; in^2 \; per \; bar$ $\qquad$ (A.5.4)

Top width: $b_t = 6.0 \; in$ $\qquad$ (A.5.5)

Bottom width: $b_b = 15 \; in$ $\qquad$ (A.5.6)

Cover: $d_c = 1.5 \; in$ $\qquad$ (A.5.7)

Bars in wall: $n_w = 4$ $\qquad$ (A.5.8)

Wall height: $h = 36 \; in$ $\qquad$ (A.5.9)

Stirrup size: #5 $\qquad$ (A.5.10)

Stirrup clearance: $d_s = 3 \; in$ $\qquad$ (A.5.11)

Stirrup spacing: $s = 8 \; in$ $\qquad$ (A.5.12)

Slope of top face: $\alpha = 4.969741 \; degrees$ $\qquad$ (A.5.13)

Slope of bottom face: $\gamma = 34.992 \; degrees$ $\qquad$ (A.5.14)

Beam Moment:

$M_b = 0 \; kip - ft$ $\qquad$ (A.5.15)

Wall Moment:

$a = \dfrac{n_b A_s f_y}{\beta_1 f_c' b} = \dfrac{(4)(0.20)(60)}{(0.85)(3.6)(36)} = 0.43573 \; in$ $\qquad$ (A.5.16)

Backside

$d_1 = b_t + (2) \tan 4.97 - 1.8125 = 4.3614 \; in$ $\qquad$ (A.5.17)

$d_2 = b_t + (12) \tan 4.97 - 1.8125 = 5.2310 \; in$ $\qquad$ (A.5.18)

$d_3 = b_t + (22) \tan 4.97 - 1.8125 = 6.1005 \; in$ $\qquad$ (A.5.19)

$d_4 = b_t + (30) \tan 4.97 - 1.8125 = 6.7962 \; in$ $\qquad$ (A.5.20)

$M_1 = A_s f_y \left(d_1 - \dfrac{a}{2} \right) = (0.20)(60) \left(4.3614 - \dfrac{0.43573}{2} \right) = 49.72 \; k - in$ $\qquad$ (A.5.21)

$M_2 = A_s f_y \left(d_2 - \dfrac{a}{2} \right) = (0.20)(60) \left(5.2310 - \dfrac{0.43573}{2} \right) = 60.16 \; k - in$ $\qquad$ (A.5.22)

$$M_3 = A_s f_y \left(d_3 - \frac{a}{2}\right) = (0.20)(60)\left(6.1005 - \frac{0.43573}{2}\right) = 70.59 \ k - in \tag{A.5.23}$$

$$M_4 = A_s f_y \left(d_4 - \frac{a}{2}\right) = (0.20)(60)\left(6.7962 - \frac{0.43573}{2}\right) = 78.94 \ k - in \tag{A.5.24}$$

$$M_N = \sum M_i = 259.41 \ kip - in \tag{A.5.25}$$

Frontside

$$d_1 = b_t + (2)\tan 4.97 - 1.8125 = 4.3614 \ in \tag{A.5.26}$$

$$d_2 = b_t + (12)\tan 4.97 - 1.8125 = 5.2310 \ in \tag{A.5.27}$$

$$d_3 = b_t + (22)\tan 4.97 - 1.8125 = 6.1005 \ in \tag{A.5.28}$$

$$d_4 = 15 - \left(\frac{3}{10}\right)(7) - 1.8125 = 11.0875 \ in \tag{A.5.29}$$

$$M_1 = A_s f_y \left(d_1 - \frac{a}{2}\right) = (0.20)(60)\left(4.3614 - \frac{0.43573}{2}\right) = 49.72 \ k - in \tag{A.5.30}$$

$$M_2 = A_s f_y \left(d_2 - \frac{a}{2}\right) = (0.20)(60)\left(5.2310 - \frac{0.43573}{2}\right) = 60.16 \ k - in \tag{A.5.31}$$

$$M_3 = A_s f_y \left(d_3 - \frac{a}{2}\right) = (0.20)(60)\left(6.1005 - \frac{0.43573}{2}\right) = 70.59 \ k - in \tag{A.5.32}$$

$$M_4 = A_s f_y \left(d_4 - \frac{a}{2}\right) = (0.20)(60)\left(11.0875 - \frac{0.43573}{2}\right) = 130.44 \ k - in \tag{A.5.33}$$

$$M_N = \sum M_i = 310.91 \ kip - in \tag{A.5.34}$$

$$M_w = \frac{\min M_N}{h} = \frac{259.41}{36} = 7.21 \ \frac{kip-ft}{ft} \tag{A.5.35}$$

Cantilever Moment:

$$a = \frac{n_b A_s f_y}{\beta_1 f_c' b} = \frac{(1)(0.31)(60)}{(0.85)(3.6)(8)} = 0.759804 \ in \tag{A.5.36}$$

Bottom Section

$$d_c = 15 - 2.86 = 11.2378 \ in \tag{A.5.37}$$

$$M_N = A_s f_y \left(d - \frac{a}{2}\right) = (0.31)(60)\left(11.2378 - \frac{0.759804}{2}\right) = 201.96 \ k - in \tag{A.5.38}$$

Top Section

$$d_c = 5.35598 \ in \tag{A.5.39}$$

$$M_N = A_s f_y \left(d - \frac{a}{2}\right) = (0.31)(60)\left(5.35598 - \frac{0.759804}{2}\right) = 92.56 \ k - in \tag{A.5.40}$$

$$M_c = \frac{\min M_N}{s} = \frac{92.56}{8} = 11.57 \ \frac{kip-ft}{ft} \tag{A.5.41}$$

6.   New Jersey Shape – 42"

<u>Given:</u>

$$f_y = 60 \ ksi \tag{A.6.1}$$

$$f_c' = 3.6 \ ksi \tag{A.6.2}$$

Rebar size: #4 $\tag{A.6.3}$

$$A_s = 0.20 \ in^2 \ per \ bar \tag{A.6.4}$$

Top width: $b_t = 6.0 \ in$ $\tag{A.6.5}$

Bottom width: $b_b = 15 \ in$ $\tag{A.6.6}$

Cover: $d_c = 1.5 \ in$ $\tag{A.6.7}$

Bars in wall: $n_w = 5$ $\tag{A.6.8}$

Wall height: $h = 42 \ in$ $\tag{A.6.9}$

Stirrup size: #5 $\tag{A.6.10}$

Stirrup clearance: $d_s = 3 \ in$ $\tag{A.6.11}$

Stirrup spacing: $s = 8 \ in$ $\tag{A.6.12}$

Slope of top face: $\alpha = 3.945186 \ degrees$ $\tag{A.6.13}$

Slope of bottom face: $\gamma = 34.992 \ degrees$ $\tag{A.6.14}$

<u>Beam Moment:</u>

$$M_b = 0 \ kip - ft \tag{A.6.15}$$

<u>Wall Moment:</u>

$$a = \frac{n_b A_s f_y}{\beta_1 f_c' b} = \frac{(5)(0.20)(60)}{(0.85)(3.6)(42)} = 0.466853 \ in \tag{A.6.16}$$

Backside

$$d_1 = b_t + (2) \tan 3.95 - 1.8125 = 4.3254 \ in \tag{A.6.17}$$

$$d_2 = b_t + (10.25) \tan 3.95 - 1.8125 = 4.8944 \ in \tag{A.6.18}$$

$$d_3 = b_t + (18.5) \tan 3.95 - 1.8125 = 5.4634 \ in \tag{A.6.19}$$

$$d_4 = b_t + (26.75) \tan 3.95 - 1.8125 = 6.0323 \ in \tag{A.6.20}$$

$$d_5 = b_t + (35) \tan 3.95 - 1.8125 = 6.6013 \ in \tag{A.6.21}$$

$$M_1 = A_s f_y \left(d_1 - \frac{a}{2} \right) = (0.20)(60) \left(4.3254 - \frac{0.466853}{2} \right) = 49.10 \ k - in \tag{A.6.22}$$

$$M_2 = A_s f_y \left(d_2 - \frac{a}{2} \right) = (0.20)(60) \left(4.8944 - \frac{0.466853}{2} \right) = 55.93 \; k - in \tag{A.6.23}$$

$$M_3 = A_s f_y \left(d_3 - \frac{a}{2} \right) = (0.20)(60) \left(5.4634 - \frac{0.466853}{2} \right) = 62.76 \; k - in \tag{A.6.24}$$

$$M_4 = A_s f_y \left(d_4 - \frac{a}{2} \right) = (0.20)(60) \left(6.0323 - \frac{0.466853}{2} \right) = 69.59 \; k - in \tag{A.6.25}$$

$$M_5 = A_s f_y \left(d_5 - \frac{a}{2} \right) = (0.20)(60) \left(6.6013 - \frac{0.466853}{2} \right) = 76.41 \; k - in \tag{A.6.26}$$

$$M_N = \sum M_i = 313.80 \; kip - in \tag{A.6.27}$$

Frontside

$$d_1 = b_t + (2) \tan 3.95 - 1.8125 = 4.3254 \; in \tag{A.6.28}$$

$$d_2 = b_t + (10.25) \tan 3.95 - 1.8125 = 4.8944 \; in \tag{A.6.29}$$

$$d_3 = b_t + (18.5) \tan 3.95 - 1.8125 = 5.4634 \; in \tag{A.6.30}$$

$$d_4 = b_t + (26.75) \tan 3.95 - 1.8125 = 6.0323 \; in \tag{A.6.31}$$

$$d_5 = 15 - \left(\frac{3.804}{10} \right) (7) - 1.8125 = 10.525 \; in \tag{A.6.32}$$

$$M_1 = A_s f_y \left(d_1 - \frac{a}{2} \right) = (0.20)(60) \left(4.3254 - \frac{0.466853}{2} \right) = 49.10 \; k - in \tag{A.6.33}$$

$$M_2 = A_s f_y \left(d_2 - \frac{a}{2} \right) = (0.20)(60) \left(4.8944 - \frac{0.466853}{2} \right) = 55.93 \; k - in \tag{A.6.34}$$

$$M_3 = A_s f_y \left(d_3 - \frac{a}{2} \right) = (0.20)(60) \left(5.4634 - \frac{0.466853}{2} \right) = 62.76 \; k - in \tag{A.6.35}$$

$$M_4 = A_s f_y \left(d_4 - \frac{a}{2} \right) = (0.20)(60) \left(6.0323 - \frac{0.466853}{2} \right) = 69.59 \; k - in \tag{A.6.36}$$

$$M_5 = A_s f_y \left(d_5 - \frac{a}{2} \right) = (0.20)(60) \left(10.525 - \frac{0.466853}{2} \right) = 123.50 \; k - in \tag{A.6.37}$$

$$M_N = \sum M_i = 360.88 \; kip - in \tag{A.6.38}$$

$$M_w = \frac{\min M_N}{h} = \frac{313.80}{42} = 7.47 \; \frac{kip - ft}{ft} \tag{A.6.39}$$

Cantilever Moment:

$$a = \frac{n_b A_s f_y}{\beta_1 f_c' b} = \frac{(1)(0.31)(60)}{(0.85)(3.6)(8)} = 0.759804 \; in \tag{A.6.40}$$

Bottom Section

$$d_c = 15 - 2.86 = 11.2378 \; in \tag{A.6.41}$$

$$M_N = A_s f_y \left(d - \frac{a}{2} \right) = (0.31)(60) \left(11.2378 - \frac{0.759804}{2} \right) = 201.96 \; k - in \tag{A.6.42}$$

Top Section

$$d_c = 5.35598 \; in \tag{A.6.43}$$

$$M_N = A_s f_y \left(d - \frac{a}{2} \right) = (0.31)(60) \left(5.35598 - \frac{0.759804}{2} \right) = 92.56 \, k - in \qquad \text{(A.6.44)}$$

$$M_c = \frac{\min M_N}{s} = \frac{92.56}{8} = 11.57 \, \frac{kip-ft}{ft} \qquad \text{(A.6.45)}$$

7. New Jersey Shape – 54"

<u>Given:</u>

$$f_y = 60 \ ksi \tag{A.6.1}$$

$$f_c' = 3.6 \ ksi \tag{A.6.2}$$

Rebar size: #5 $\hspace{10cm}$ (A.6.3)

$$A_s = 0.31 \ in^2 \ per \ bar \tag{A.6.4}$$

Top width: $b_t = 8.0 \ in$ $\hspace{8cm}$ (A.6.5)

Bottom width: $b_b = 17.5 \ in$ $\hspace{7cm}$ (A.6.6)

Cover: $d_c = 1.5 \ in$ $\hspace{9cm}$ (A.6.7)

Bars in wall: $n_w = 7$ $\hspace{9cm}$ (A.6.8)

Wall height: $h = 54 \ in$ $\hspace{8.5cm}$ (A.6.9)

Stirrup size: #5 $\hspace{9cm}$ (A.6.10)

Stirrup clearance: $d_s = 3 \ in$ $\hspace{7.5cm}$ (A.6.11)

Stirrup spacing: $s = 12 \ in$ $\hspace{8cm}$ (A.6.12)

Slope of top face: $\alpha = 3.945186 \ degrees$ $\hspace{5cm}$ (A.6.13)

Slope of bottom face: $\gamma = 34.992 \ degrees$ $\hspace{5.5cm}$ (A.6.14)

<u>Beam Moment:</u>

$$M_b = 0 \ kip - ft \tag{A.6.15}$$

<u>Wall Moment:</u>

$$a = \frac{n_b A_s f_y}{\beta_1 f_c' b} = \frac{(7)(0.31)(60)}{(0.85)(3.6)(54)} = 0.779801 \ in \tag{A.6.16}$$

Backside

$$d_1 = 6.5 \ in \tag{A.6.17}$$

$$d_2 = 6.86 \ in \tag{A.6.18}$$

$$d_3 = 7.4 \ in \tag{A.6.19}$$

$$d_4 = 7.76 \ in \tag{A.6.20}$$

$$d_5 = 8.12 \ in \tag{A.6.21}$$

$$d_6 = 8.48 \ in \tag{A.6.20}$$

$$d_7 = 9.2 \ in \tag{A.6.21}$$

$$M_1 = A_s f_y \left(d_1 - \frac{a}{2}\right) = (0.20)(60)\left(6.5 - \frac{0.779801}{2}\right) = 112.47 \; k-in \tag{A.6.22}$$

$$M_2 = A_s f_y \left(d_2 - \frac{a}{2}\right) = (0.20)(60)\left(6.86 - \frac{0.779801}{2}\right) = 119.10 \; k-in \tag{A.6.23}$$

$$M_3 = A_s f_y \left(d_3 - \frac{a}{2}\right) = (0.20)(60)\left(7.4 - \frac{0.779801}{2}\right) = 129.04 \; k-in \tag{A.6.24}$$

$$M_4 = A_s f_y \left(d_4 - \frac{a}{2}\right) = (0.20)(60)\left(7.76 - \frac{0.779801}{2}\right) = 135.67 \; k-in \tag{A.6.25}$$

$$M_5 = A_s f_y \left(d_5 - \frac{a}{2}\right) = (0.20)(60)\left(8.12 - \frac{0.779801}{2}\right) = 142.29 \; k-in \tag{A.6.26}$$

$$M_6 = A_s f_y \left(d_4 - \frac{a}{2}\right) = (0.20)(60)\left(8.48 - \frac{0.779801}{2}\right) = 148.92 \; k-in \tag{A.6.25}$$

$$M_7 = A_s f_y \left(d_5 - \frac{a}{2}\right) = (0.20)(60)\left(9.2 - \frac{0.779801}{2}\right) = 162.17 \; k-in \tag{A.6.26}$$

$$M_N = \sum M_i = 949.67 \; kip-in \tag{A.6.27}$$

Frontside

$$d_7 = 13.7 \; in \tag{A.7..}$$

$$M_7 = A_s f_y \left(d_5 - \frac{a}{2}\right) = (0.20)(60)\left(13.7 - \frac{0.779801}{2}\right) = 245.01 \; k-in \tag{A.6.26}$$

$$M_N = \sum M_i = 1{,}032.51 \; kip-in \tag{A.6.38}$$

$$M_w = \frac{\min M_N}{h} = \frac{949.67}{54} = 17.59 \; \frac{kip-ft}{ft} \tag{A.6.39}$$

Cantilever Moment:

$$a = \frac{A_s f_y}{\beta_1 f_c' b} = \frac{(0.31)(60)}{(0.85)(3.6)(12)} = 0.506536 \; in \tag{A.6.40}$$

Bottom Section

$$d_c = 9.8 \; in \tag{A.6.41}$$

$$M_N = A_s f_y \left(d - \frac{a}{2}\right) = (0.31)(60)\left(9.8 - \frac{0.506536}{2}\right) = 177.57 \; k-in \tag{A.6.42}$$

Top Section

$$d_c = 8.48 \; in \tag{A.6.43}$$

$$M_N = A_s f_y \left(d - \frac{a}{2}\right) = (0.31)(60)\left(8.48 - \frac{0.506536}{2}\right) = 151.44 \; k-in \tag{A.6.44}$$

$$M_c = \frac{\min M_N}{s} = \frac{151.44}{12} = 12.62 \; \frac{kip-ft}{ft} \tag{A.6.45}$$

END OF DOCUMENT